Supplement of Atmos. Chem. Phys., 25, 14735–14745, 2025
https://doi.org/10.5194/acp-25-14735-2025-supplement

Atmospheric Chemistry and Physics
Open Access

Supplement of

Characteristics, main sources, health risks of $PM_{2.5}$-bound polyfluoroalkyl substances (PFAS) in Zhengzhou, central China: from seasonal variation perspective

Jingshen Zhang et al.

Correspondence to: Xibin Ma (maxibin163@163.com) and Nan Jiang (jiangn@zzu.edu.cn)

S1. Experiment

S1.1 Samples Analysis

S1.1.1 Samples Pretreatment

1): Quartz filters were cut into small pieces and placed into 50 mL polypropylene (PP) centrifuge tubes. An internal standard mixture solution of 50 μL at 0.2 μg/mL was added to the cut filters.

2): Organic solvents (methanol, HPLC grade) were added to extract polyfluoroalkyl substances (PFAS) from the samples via ultrasonic extraction. The ultrasonic extraction process was conducted in three stages. Initially, 4 mL of methanol was added and the samples were sonicated for 20 minutes; subsequently, 3 mL of methanol was added for another 20 minutes of sonication; finally, an additional 3 mL of methanol was added for a 10-minute extraction. The extracts from each sonication were collected separately.

3): The extracts were diluted with ultrapure water to a total volume of 250 mL and then centrifuged (4500 r/min for 15 minutes) to obtain the clear supernatant.

4): The clear supernatant was enriched using a solid-phase extraction (SPE) instrument with a wax SPE column (6 mL, 150 mg). The first step involved conditioning the column with 4 mL of 0.1% aqueous ammonia-methanol solution, followed by 4 mL of methanol and 4 mL of ultrapure water; the second step was loading the 250 mL supernatant onto the wax SPE column at a flow rate of 1-2 drops per second; the third step involved washing with 4 mL of 25 mM ammonium acetate solution (pH=4); the fourth step was drying under vacuum for 30 minutes using the SPE instrument; the fifth step was elution with 4 mL of methanol followed by 4 mL of 0.1% aqueous ammonia-methanol solution, and the eluate was collected in a 10 mL PP centrifuge tube to obtain 8 mL of the final eluate.

5): Nitrogen Evaporation was performed using a nitrogen evaporator to completely dry the eluate (the nitrogen blow temperature should not exceed 40°C, and no bubbles should be present on the liquid surface).

6): The dried eluate was reconstituted with 1 mL of methanol.

7): The reconstituted 1 mL solution was filtered through a 0.22 μm nylon syringe filter into a 2 mL brown sample vial for subsequent chromatographic analysis.

S1.1.2 Mass spectrometer condition

Chromatographic Column Selection: A C18 reverse-phase column (150 mm × 2.1 mm, 1.8 μm) was used. Chromatographic Conditions: Mobile phase A (2 mM ammonium acetate aqueous solution); Mobile phase B (acetonitrile); runtime of 20 minutes; flow rate of 0.3 mL/min; column temperature of 40°C; injection volume of 10 μL; gradient elution program (0–14 min 80% A, 14–16 min 10% A, 16–20 min 80% A).

Mass Spectrometry Conditions: Electrospray ionization (ESI) source in negative ion mode. Detection mode: Multiple Reaction Monitoring (MRM). Curtain gas pressure at 35.0 psi; spray voltage at –4500 V; nebulizer temperature at 550°C; nebulizer gas pressure at 55 psi; auxiliary gas pressure at 60 psi.

S1.1.3 Material analysis

Qualitative Analysis: One precursor ion and two product ions were selected for monitoring the target compounds. Under the same experimental conditions, the absolute value of the relative deviation between the retention time of the target compound in the sample and that in the standard sample should be less than 2.5%; and the relative abundance of the qualitative product ions (K_{sam}) of the target compound in the sample compared with the relative abundance of the corresponding qualitative product ions (K_{std}) in a standard solution of similar

concentration should not exceed the specified range, thus confirming the presence of the corresponding target compound in the sample.

$$K_{sam} = \frac{A_2}{A_1} \times 100\% \quad \text{(S1)}$$

Where:

K_{sam} is the relative abundance of the qualitative product ions of the target compound in the sample, %;

A2 is the response value of the secondary mass spectrometry qualitative product ions of the target compound in the sample;

A_1 is the response value of the secondary mass spectrometry quantitative precursor ions of the target compound in the sample.

$$K_{std} = \frac{A_{std2}}{A_{std1}} \times 100\% \quad \text{(S2)}$$

Where:

K_{std} is the relative abundance ratio of the qualitative product ions of the target compound in the standard sample, %;

A_{std2} is the response value of the secondary mass spectrometry qualitative product ions of the target compound in the standard sample;

A_{std1} is the response value of the secondary mass spectrometry quantitative precursor ions of the target compound in the standard sample.

K_{std} (%)	K_{sam} Tolerated Deviation (%)
$K_{std} > 50$	±20
$20 < K_{std} \leq 50$	±25
$10 < K_{std} \leq 20$	±30
$K_{std} \leq 10$	±50

The mass concentrations of 17 perfluoro compounds in the samples were calculated using the following formula:

$$\rho_i = \frac{x_i \times m_{is}}{V_w} \quad \text{(S3)}$$

Where:

ρ_i is the mass concentration of the ith perfluoro compound in the sample;

x_i is the concentration ratio of the ith perfluoro compound to the corresponding internal standard calculated from the calibration curve;

m_{is} is the added mass of the internal standard corresponding to the ith perfluoro compound;

V_w is the sample volume.

S1.2 Source Apportionment

The PMF model, which is widely applied as a receptor model (Paatero, 1997; Paatero and Tapper, 1994), divides the sample data matrix into two (factor contribution (G) and feature profile (F)) to quantitatively identify the source of contaminants. The factor contributions and profiles were derived via the PMF model by minimizing the objective function Q.

The two matrices (factor contributions (G) and factor profiles (F)), as described in the following:

$$X=G\times F+E \tag{S4}$$

where X, the data matrix, is the n×m matrix of the m measured chemical species in *n* samples; F is a p×m–matrix with rows that represent the emission profiles of p factors; and G, an n×p–matrix with columns that represent the scores of p factors. Matrix E is the residual matrix.

Factor contributions and profiles were derived by the PMF model by minimizing the objective function Q, as described in the following:

$$Q=\sum_{i=1}^{n}\sum_{j=1}^{m}\left[\frac{e_{ij}}{u_{ij}}\right]^2 \tag{S5}$$

where e_{ij} is the residual of the j_{th} chemical component in the i_{th} sample, and u_{ij} is the uncertainty of the j_{th} chemical component in the i_{th} sample.

According to the previous studies (Jiang et al., 2018), uncertainty is calculated as follows:

$$u_{ij} = \begin{cases} 0.2 * c_{ij} + MDL/3 & u_{ij} \le MLD \\ 0.1 * c_{ij} + MDL/3 & u_{ij} > MLD \end{cases} \quad \text{(S6)}$$

where u_{ij} is the uncertainty of the j_{th} chemical component in the i_{th} sample, c_{th} is the concentration of the j_{th} chemical component in the i_{th} sample. The missing data is instead by species median, and the outliers are excluded from the PMF analysis. More other details were described in the PMF 5.0 User Guide (Yu et al., 2009).

The chemical database used for the PMF consisted of PFAS, PFBA, PFPeA, PFHxA, PFHpA, PFOA, PFNA, PFDA, PFUnDA, PFDoDA, PFTrDA, PFTeDA, PFHxDA, PFODA, PFBS, PFHxS, PFOS, PFDS, giving a total of 22 species. In this study, the overall number of samples and the number of variables complies with the ratio of at least 3/1, as proposed by Belis et al (Belis et al., 2015).

All the included species were defined from weak to strong in the PMF based on their signal-to-noise ratio (S/N). The PM species were categorized as “bad” when the S/N ratio were below 0.2; “weak” when the S/N ratio were between 0.2 and 2; and “strong” when the S/N ratio were higher than 2 (Esmaeilirad et al., 2020). The bad species are excluded from the analysis while the uncertainty for the weak species is tripled. PFAS was defined as a “total variable” and was automatically categorized as “weak”. All the included species were well reconstructed and were qualified as “strong”.

The program was run several times to find the smallest value of Q_{expect} and to reduce the observed value of residual error matrix E as much as possible in order to ensure that the simulation results show a good correlation with the observations. The stability of a PMF solution was estimated based on the bootstrap (BS), displacement (DISP), and BS-DISP results (US EPA., 2014). After running the program several times, the number of sources was set from two to six, and the results of four sources were selected due to their adequate fit to the measurement data and their physical

meaning (more details can be found in Table S2). When the DISP analysis results were 4 factors, no factor exchange occurred, indicating that the results were relatively stable. Each factor mapping of the 4 factor results of BS analysis is greater than 80%, indicating that the uncertainty of BS is acceptable and the number of factors is reasonable. The PMF results were constrained with dQrobust of 0.59% and Fpeak = 0.0 produced the most physically reasonable source profiles.

S1.3 Average Daily Inhalation (ADI) and Estimated Daily Intake (EDI) Calculation

Median concentrations were utilized for data analysis in lieu of mean values, a choice necessitated by the presence of extreme values (Huang et al., 2021). Reference-based methods were employed to calculate the EDI and annual exposure dosages (AEDs) for adults (Liu et al., 2017; Liu et al., 2023). The two calculations are as follows:

$$\mathrm{ADI} = \frac{\rho \times \mathrm{IR} \times \mathrm{EF} \times \mathrm{ED}}{\mathrm{BW} \times \mathrm{AT}} \quad \text{(S7)}$$

$$\mathrm{EDI} = \rho \times \mathrm{IR} \quad \text{(S8)}$$

$$\mathrm{AED} = \mathrm{EDI} \times \mathrm{EF} \times \mathrm{DR} \quad \text{(S9)}$$

where ADI is average daily inhalation ($pg \cdot (kg \cdot d)^{-1}$), ρ is the daily concentration of each PFAS ($pg \cdot m^{-3}$), IR is the adult inhalation rate (15.73 $m^3 \cdot day^{-1}$), EF is the annual exposure frequency (350 $days \cdot year^{-1}$, without the time of two-week annual vacation), ED is exposure duration (72 a), BW is adult weight (65.0 kg), AT is average time (72 $a \cdot 365\ d \cdot a^{-1}$), EDI is estimated daily intake (pg), and DR is the detection rate of the compound.

S2. Tabulation

Table. S1. PFAS CAS and corresponding internal standard substance

Compound	CAS	Internal Standard	Relative Molecular Mass	Retention time (min)
PFBA	375-22-4	$^{13}C_4$PFBA	214.04	2.7
PFPeA	2706-90-3	$^{13}C_4$PFBA	264.05	3.9
PFHxA	307-24-4	$^{13}C_4$PFHxA	314.06	5.1
PFHpA	375-85-9	$^{13}C_4$PFHxA	364.07	5.4
PFOA	335-67-1	$^{13}C_4$PFOA	414.08	6.1
PFNA	375-95-1	$^{13}C_4$PFNA	464.09	6.9
PFDA	335-76-2	$^{13}C_4$PFDA	514.10	7.5
PFUnDA	2058-94-8	$^{13}C_4$PFUnDA	564.11	7.8
PFDoDA	307-55-1	$^{13}C_2$PFDoDA	614.12	8.6
PFTrDA	72629-94-8	$^{13}C_2$PFDoDA	664.13	9.2
PFTeDA	376-06-7	$^{13}C_2$PFDoDA	714.14	9.4
PFHxDA	67905-19-5	$^{13}C_2$PFDoDA	814.16	10.2
PFODA	16517-11-6	$^{13}C_2$PFDoDA	914.18	10.8
PFBS	375-73-5	$^{18}O_2$PFHxS	300.11	11.0
PFHxS	355-46-4	$^{18}O_2$PFHxS	400.14	11.8
PFOS	1763-23-1	$^{13}C_4$PFOS	500.16	13.2
PFDS	335-77-3	$^{13}C_4$PFOS	600.18	14.4
$^{13}C_4$PFBA			226.04	2.7
$^{13}C_4$PFHxA			326.04	5.1
$^{13}C_4$PFOA			426.05	6.9
$^{13}C_4$PFNA			476.06	7.5
$^{13}C_4$PFDA			526.07	7.8
$^{13}C_4$PFUnDA			576.08	8.6
$^{13}C_2$PFDoDA			626.09	9.2
$^{18}O_2$PFHxS			402.10	9.4
$^{13}C_4$PFOS			526.08	10.2

Table. S2. PFAS standard and corresponding internal standard substances and test information

Compound	Internal Standard	Standard (internal standard) Precursor Ion（m/z）	Standard (internal standard) Product Ion（m/z）	Standard (internal standard) DP（V）	Standard (internal standard) CE（V）	Mark recovery（%）	MDL（$ng \cdot L^{-1}$）
PFBA	$^{13}C_4$PFBA	213（217）	169（172）	–40（–50）	–13（–12）	97.49–112.02	0.3
PFPeA	$^{13}C_4$PFBA	263（217）	219/69（172）	–40（–50）	–10/–50（–12）	73.61–112.98	0.2
PFHxA	$^{13}C_4$PFHxA	313（315）	269/119（270）	–45（–55）	–13/–27（–14）	94.84–115.89	0.2
PFHpA	$^{13}C_4$PFHxA	363（315）	319/169（270）	–30（–55）	–14/–24（–14）	71.74–111.84	0.2
PFOA	$^{13}C_4$PFOA	413（417）	369/169（372）	–40（–70）	–14/–24（–20）	91.04–117.75	0.3
PFNA	$^{13}C_4$PFNA	463（468）	419/169（423）	–35（–70）	–16/–24（–22）	92.55–112.96	0.2
PFDA	$^{13}C_4$PFDA	513（515）	469/219（470）	–40（–75）	–18/–26（–17）	96.81–115.60	0.2
PFUnDA	$^{13}C_4$PFUnDA	563（565）	519/319（520）	–70（–60）	–16/–28（–15）	96.81–115.24	0.2
PFDoDA	$^{13}C_2$PFDoDA	613（615）	569/169（570）	–70（–60）	–18/–36（–15）	97.46–116.71	0.2
PFTrDA	$^{13}C_2$PFDoDA	663（615）	619/169（570）	–65（–60）	–20/–38（–15）	96.88–110.99	0.3
PFTeDA	$^{13}C_2$PFDoDA	713（615）	669/169（570）	–85（–60）	–20/–38（–15）	98.10–113.01	0.2
PFHxDA	$^{13}C_2$PFDoDA	813（615）	769/169（570）	–90（–60）	–18/–30（–15）	99.38–118.08	0.3
PFODA	$^{13}C_2$PFDoDA	913（615）	869/169（570）	–40（–60）	–25/–45（–15）	85.64–104.97	0.2
PFBS	$^{18}O_2$PFHxS	299（403）	80/99（103）	–90（–90）	–70/–38（–75）	71.27–106.25	0.3
PFHxS	$^{18}O_2$PFHxS	399（403）	80/99（103）	–90（–90）	–90/–72（–75）	89.91–102.78	0.3
PFOS	$^{13}C_4$PFOS	499（503）	80/99（80）	–105（–90）	–110/–98（–95）	96.42–111.07	0.3
PFDS	$^{13}C_4$PFOS	599（503）	80/99（80）	–120（–90）	–124/–110（–95）	97.56–109.07	0.2

Table. S3. Summary of PMF and error estimation diagnostics from two to six factors

	PMF				
Factor number	2	3	4	5	6
Q_{robust}	15289	11948	11021	9936	7941
Q_{true}	21987	16238	13123	11071	9375
$Q_{expected}$	1480	1301	1219	1189	1048
$Q_{true}/Q_{expected}$	14.85608108	12.48117	10.76538	9.311186	8.945611
$Q_{robust}/Q_{expected}$	10.33040541	9.183705	9.041017	8.356602	7.57729
DISP%dQ	0	0	0	0	0
DISP swaps	0	0	0	0	0
Factor with BS mapping < 80%	All factor > 80%	factor 3, 47%	All factor > 80%	factor 3, 65%, factor 4, 33%,	factor 1, 41%, factor 5, 63%, factor 6, 71%

Table. S4. Atmospheric $PM_{2.5}$ sample information table

Sampling time	Samples quantity	Sampling volume (m^3)	Membrane diameter (mm)	Sample type
Spring	15	3.25	90	Urban atmospheric $PM_{2.5}$ sample
Summer	15	3.25	90	
Autumn	15	3.25	90	
Winter	15	3.25	90	

S3. Figure

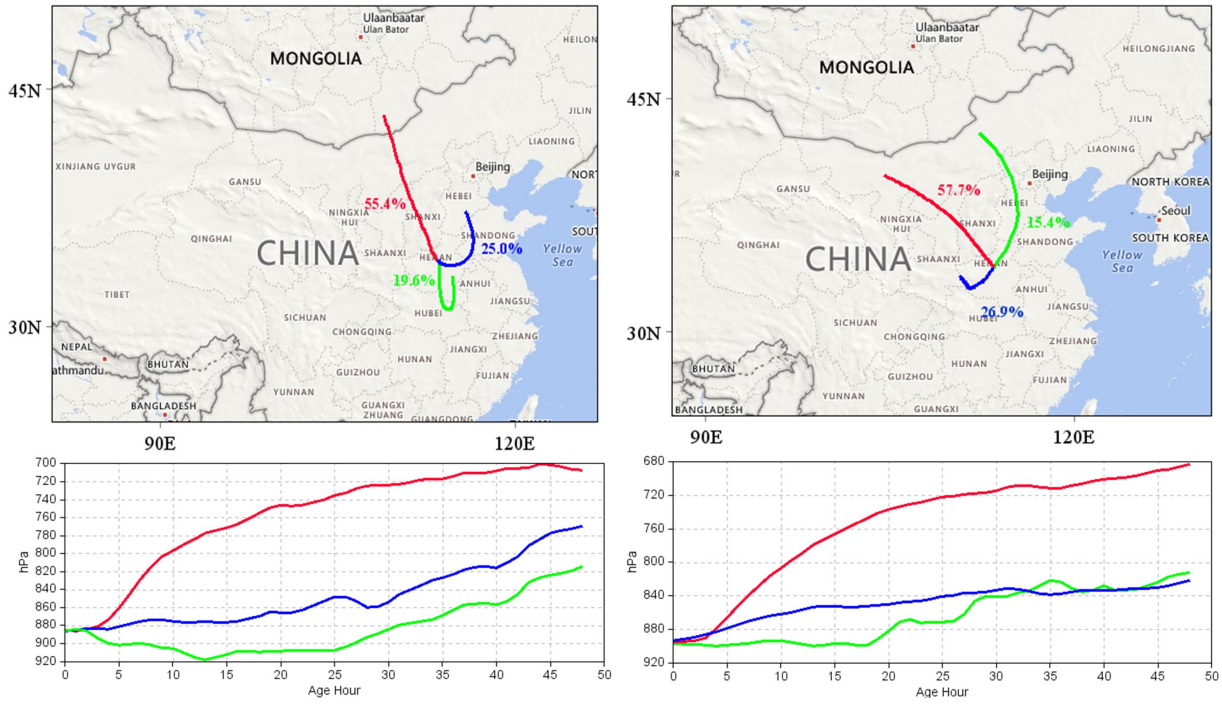

Fig. S1. Cluster analysis map of backward trajectories in Zhengzhou City (left and right are summer and autumn respectively,created by MeteoInfoMap 3.5.11 (Wang, 2014; Wang, 2019)). © Microsoft. The software is open.

References

Belis, C.A., Karagulian, F., Amato, F., Almeida, M., Artaxo, P., Beddows, D.C.S., Bernardoni, V., Bove, M.C., Carbone, S., Cesari, D., Contini, D., Cuccia, E., Diapouli, E., Eleftheriadis, K., Favez, O., El Haddad, I., Harrison, R.M., Hellebust, S., Hovorka, J., Jang, E., Jorquera, H., Kammermeier, T., Karl, M., Lucarelli, F., Mooibroek, D., Nava, S., Nojgaard, J.K., Paatero, P., Pandolfi, M., Perrone, M.G., Petit, J.E., Pietrodangelo, A., Pokorna, P., Prati, P., Prevot, A.S.H., Quass, U., Querol, X., Saraga, D., Sciare, J., Sfetsos, A., Valli, G., Vecchi, R., Vestenius, M., Yubero, E., and Hopke, P.K.: A new methodology to assess the performance and uncertainty of source apportionment models II: The results of two European intercomparison exercises, Atmos. Environ., 123, 240-250, http://dx.doi.org/10.1016/j.atmosenv.2015.10.068, 2015.

Esmaeilirad, S., Lai, A., Abbaszade, G., Schnelle-Kreis, J., Zimmermann, R., Uzu, G., Daellenbach, K., Canonaco, F., Hassankhany, H., Arhami, M., Baltensperger, U., Prévôt, A.S.H., Schauer, J.J., Jaffrezo, J.L., Hosseini, V., and El Haddad, I.: Source apportionment of fine particulate matter in a Middle Eastern Metropolis, Tehran-Iran, using PMF with organic and inorganic markers, Sci. Total. Environ., 705, http://dx.doi.org/10.1016/j.scitotenv.2019.135330, 2020.

Huang, W., Shi, Y.M., Huang, J.L., Deng, C.L., Tang, S.Q., Liu, X.T., and Chen, D.: Occurrence of Substituted ρ-Phenylenediamine Antioxidants in Dusts, Environ. Sci. Technol. Lett., 8, 381-385. http://dx.doi.org/10.1021/acs.estlett.1c00148, 2021.

Jiang, N., Yin, S.S., Guo, Y., Li, J.Y., Kang, P.R., Zhang, R.Q., and Tang, X.Y.: Characteristics of mass concentration, chemical composition, source apportionment of $PM_{2.5}$ and PM_{10} and health risk assessment in the emerging megacity in China, Atmos. Pollut. Res., 9, 309-321, http://dx.doi.org/10.1016/j.apr.2017.07.005, 2018.

Liu, J., Wang, Y., Le, P.H., Shou, Y.P., Li, T., Yang, M.M., Wang, L., Yue, J.J., Yi, X.L., and Guo, L.Q.: Polycyclic Aromatic Hydrocarbons (PAHs) at High Mountain Site in North China: Concentration, Source and Health Risk Assessment, Aerosol Air Qual. Res., 17, 2867-2877, http://dx.doi.org/10.4209/aaqr.2017.08.0288, 2017.

Liu, L.S., Guo, Y.T., Wu, Q.Z., Zeeshan, M., Qin, S.J., Zeng, H.X., Lin, L.Z., Chou, W.C., Yu, Y.J., Dong, G.H., and Zeng, X.W.: Per- and polyfluoroalkyl substances in ambient fine particulate matter in the Pearl River Delta, China: Levels, distribution and health implications, Environ. Pollut., 334, http://dx.doi.org/10.1016/j.envpol.2023.122138, 2023.

Paatero, P.: Least squares formulation of robust non-negative factor analysis, Chemometrics Intell. Lab. Syst. 37, 23-35, http://dx.doi.org/10.1016/s0169-7439(96)00044-5, 1997.

Paatero, P., Tapper, U.: Positive matrix factorization - a nonnegative factor model with optimal utilization of error-estimates of data values, Environmetrics., 5, 111-126, http://dx.doi.org/10.1002/env.3170050203, 1994.

US EPA: Positive matrix factorization (PMF) 5.0 fundamentals and user guide [EB], Office of Research and Development, Washington, DC, 2014.

Wang, Y.Q.: Meteolnfo: GIS software for meteorological data visualization and analysis, Meteorol. Appl., 21, 360-368, https://doi.org/10.1002/met.1345, 2014.

Wang, Y.Q.: An Open Source Software Suite for Multi-Dimensional Meteorological Data Computation and Visualisation, Journal of Open Research Software., 7, 21, https://doi.org/10.5334/jors.267, 2019.

Yu, Y., Galle, B., Panday, A., Hodson, E., Prinn, R., and Wang, S.: Observations of high rates of NO_2-HONO conversion in the nocturnal atmospheric boundary layer in Kathmandu, Nepal, Atmos. Chem. Phys., 9, 6401-6415, http://dx.doi.org/10.5194/acp-9-6401-2009, 2009.